

LA-UR -81-1906

Los Alamos National Laboratory is operated by the University of California for the United States Department of Energy under contract W-7405-ENG-36

MASTER

TITLE A HYDROGEN STORAGE-BED DESIGN FOR TRITIUM SYSTEMS TEST ASSEMBLY

AUTHOR(S) Hattie S. Cullington, Michael G. Wheeler, and John W. McMullen

SUBMITTED TO International Symposium on Metal-Hydrogen Systems,
Miami Beach, FL, April 13-15, 1981

By acceptance of this article the publisher recognizes that the U.S. Government retains a nonexclusive, royalty-free license to publish or reproduce the published form of this contribution or to allow others to do so for U.S. Government purposes. The Los Alamos National Laboratory requests that the publisher identify this article as work performed under the auspices of the U.S. Department of Energy.

Los Alamos Los Alamos National Laboratory
Los Alamos, New Mexico 87545

62112

A HYDROGEN STORAGE-BED DESIGN
FOR TRITIUM SYSTEMS TEST ASSEMBLY

Hatice S. Cullingford, Michael G. Wheeler, and John W. McMullen
Design Engineering Division
Los Alamos National Laboratory
Los Alamos, NM 87545

ABSTRACT

The Los Alamos National Laboratory has completed the design of a hydrogen storage bed for the Tritium Systems Test Assembly (TSTA). Our objective is to store hydrogen isotopes as uranium hydrides and recover them by dehydriding. The specific use of the storage bed is to store DT gas as $U(D,T)_3$ when it is required for the TSTA.

The hydrogen storage bed consists of a primary container in which uranium powder is stored and a secondary container for a second level of safety in gas confinement. The primary container, inlet and outlet gas lines, cartridge heaters, and instrumentation are assembled in the secondary container. The design of the hydrogen storage bed is presented, along with the modeling and analysis of the bed behavior during hydriding-dehydriding cycles.

KEYWORDS

Hydrogen storage; deuterium; tritium; uranium hydride; storage beds; fusion energy.

INTRODUCTION

The Los Alamos National Laboratory is constructing a Tritium Systems Test Assembly (TSTA) for the Office of Fusion Energy of the Department of Energy. The objectives of TSTA are as follows (Anderson, 1978).

1. Develop and demonstrate all aspects of the deuterium-tritium fuel-handling cycle required for developmental fusion reactors.
2. Demonstrate and improve the reliability in tritium service of a wide variety of fusion reactor components such as valves, pumps, and instrumentation.
3. Demonstrate the routine, safe handling of tritium in significant quantities for fusion reactors.

TSTA will be the first fusion facility to charge large quantities of tritium, namely, 0.15 kg in 1982. The main systems of TSTA are shown in Fig. 1. Several storage beds are needed for the hydrogen isotopes in the system during the annual operational cycle of TSTA. The following operational modes will require hydrogen storage beds.

1. Controlled Shutdown - The contents of the distillation columns in the Isotope Separation System (ISS) will be transferred to the hydrogen storage beds after a warm-up period during a controlled shutdown of TSTA. The hydrogen isotopes will be recovered and sent back to the ISS for startup.

2. Emergency Shutdown - The hydrogen isotopes will automatically expand into a surge tank from the distillation columns in the ISS under an emergency shutdown. The surge tank contents will then be transferred to the storage beds for a short-term or a long-term shutdown.

3. Inventory Control - An inventory assay will be implemented every six months after transferring the hydrogen isotopes in the system to the storage beds. This operation will involve an Inventory Control System.

4. Line Cleanup - The flow lines of the Inventory Control System will be cleaned up by using the storage beds.

The following unique requirements are imposed on the hydrogen storage beds:

- Large DT gas loads,
- Fast loading rates,
- Pure DT gas rather than in dilution with other gases,
- DT gas mixture (nominally 50-50) rather than D_2 or T_2 ,
- Storage at room temperature, and
- Purging of 3He .

These requirements were translated to the following design criteria:

- A (developed) technology base,
- Adequate safety margins,

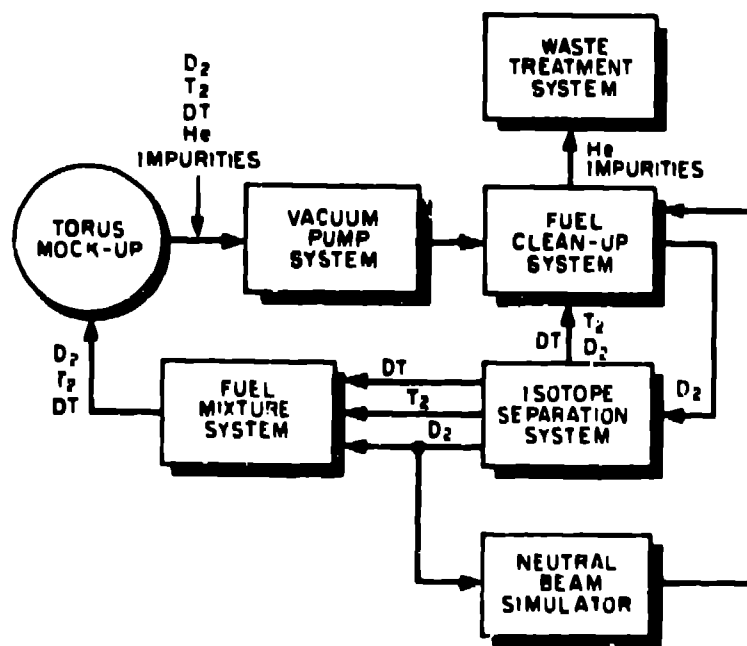


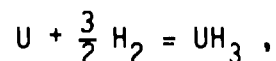
Fig. 1. Main systems of TSTA.

- Flow-through design,
- Simplicity in design and operation, and
- Double containment.

Our review of the existing technology base resulted in a decision to design a uranium bed (U-bed) for storage of hydrogen isotopes as uranium hydrides. Uranium hydride contains about twice as many hydrogen atoms per unit volume as liquid hydrogen (4.2×10^{28} atoms m^{-3} at 20°K) and can be stored at room temperature. Completely hydrided uranium has been used as a source of high-purity hydrogen since World War II (Mueller, Blackledge, and Libovitz, 1968). In addition to the research type U-beds, a number of engineered storage bed designs have been developed in the United States over the years (Singleton and Aire, 1980).¹ We will present the design of a hydrogen storage bed that meets the TSTA requirements. Supporting analyses will also be provided for the storage-recovery cycles of TSTA.

DESIGN DESCRIPTION

Figure 2 shows a cutaway view of the TSTA hydrogen storage bed. The design objective is to store hydrogen isotopes as uranium hydrides and recover the hydrogenous gases by dehydriding. The chemical reaction of importance is



where H can be H, D, or T. The kinetics and other characteristics of this reaction are well documented in the literature.

The TSTA hydrogen storage bed consists of a primary container, in which uranium powder is stored, and a secondary container for a second level of gas confinement and leak detection. The primary container houses the uranium powder in 27 cells. The cells are arranged in nine assemblies in a square array. Each assembly is formed in a bore made in a copper block. The assembly is made by stacking porous copper frits and copper pipe spacers alternately to produce three cells in a column, as illustrated in Fig. 3. Each cell contains 0.22 kg of uranium powder for hydriding. Table 1 lists the parameters for the hydrogen storage bed.

The inlet gas is distributed to the nine assemblies from an inlet plenum for hydriding. The hydrogenous gases from the dehydriding cycle collect in an outlet plenum before leaving the primary container through the outlet pipe. Thus, a gas leak in the primary containment (the primary container or in the inlet and outlet piping) would be confined in the secondary container.

Cartridge heaters are used during the dehydriding cycle to heat the uranium hydride to 723°K. The primary container, inlet and outlet gas lines, cartridge heaters, and instrumentation are hung by the support plates and rods from the cover assembly of the secondary containment.

The cover of the secondary container provides the penetrations for the gas inlet and outlet lines, the heater and thermocouple connections, the rupture disc, and a vacuum port. The rupture disc is a safety device should an unlikely event result in an overpressure of up to 0.69 MPa. The secondary container can be evacuated to insulate the primary container during a dehydriding cycle. This

¹Private communication with colleagues in Lawrence Livermore National Laboratory, Los Alamos National Laboratory, and Sandia National Laboratories-Livermore.

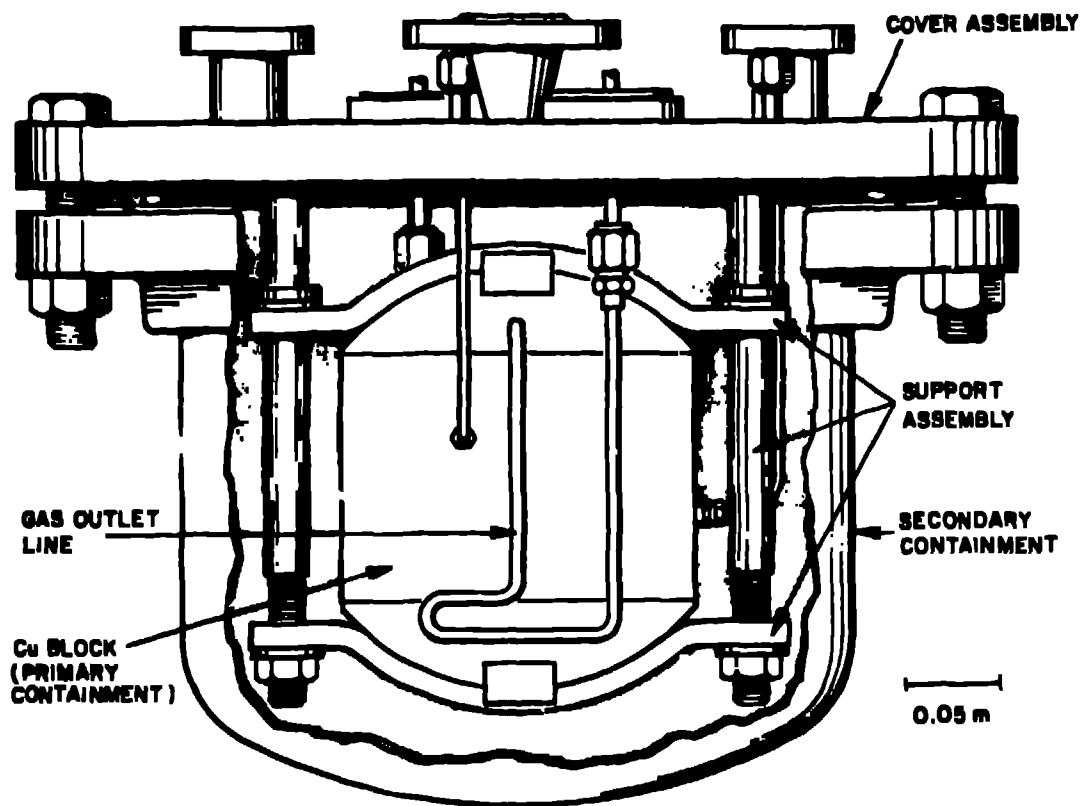


Fig. 2. Cutaway view of the TSTA hydrogen storage bed.

evacuation also can permit leak detection and handling in the case of a tritium leak from the primary to the secondary container.

All surfaces in contact with the uranium powder are oxygen-free copper. Copper was selected instead of stainless steel for the following reasons.

1. Better tritium barrier because of its lower permeability and lower solubility for tritium.
2. Better heat transfer medium because of its higher thermal conductivity.
3. Better compatibility with uranium because of a higher eutectic point than that of iron (1223 vs 998°K) (Hansen, 1965).
4. Reduced hydrogen stress cracking (reduced mechanical embrittlement or no decarburization) (Hagel and Wiska, 1980).

All load-bearing components such as the secondary container, support plates and rods, cover, and gas inlet and outlet lines are made of stainless steel type 304 (SS 304). The primary container is thermally decoupled from the support rods and the secondary container by ceramic bushings made of MACOR. Nickel foil might be used as a super insulation in the secondary container gap around the primary container. A portable vacuum pump of 50 l s⁻¹ will be used to evacuate this insulation volume to begin a recovery (dehydriding) cycle. The cartridge heaters will then start heating the copper block to 723°K.

There are two levels of safety for tritium confinement: the primary container and the secondary container for the storage process, with the piping entering or leaving the storage bed and the glovebox for gas delivery/recovery process. The

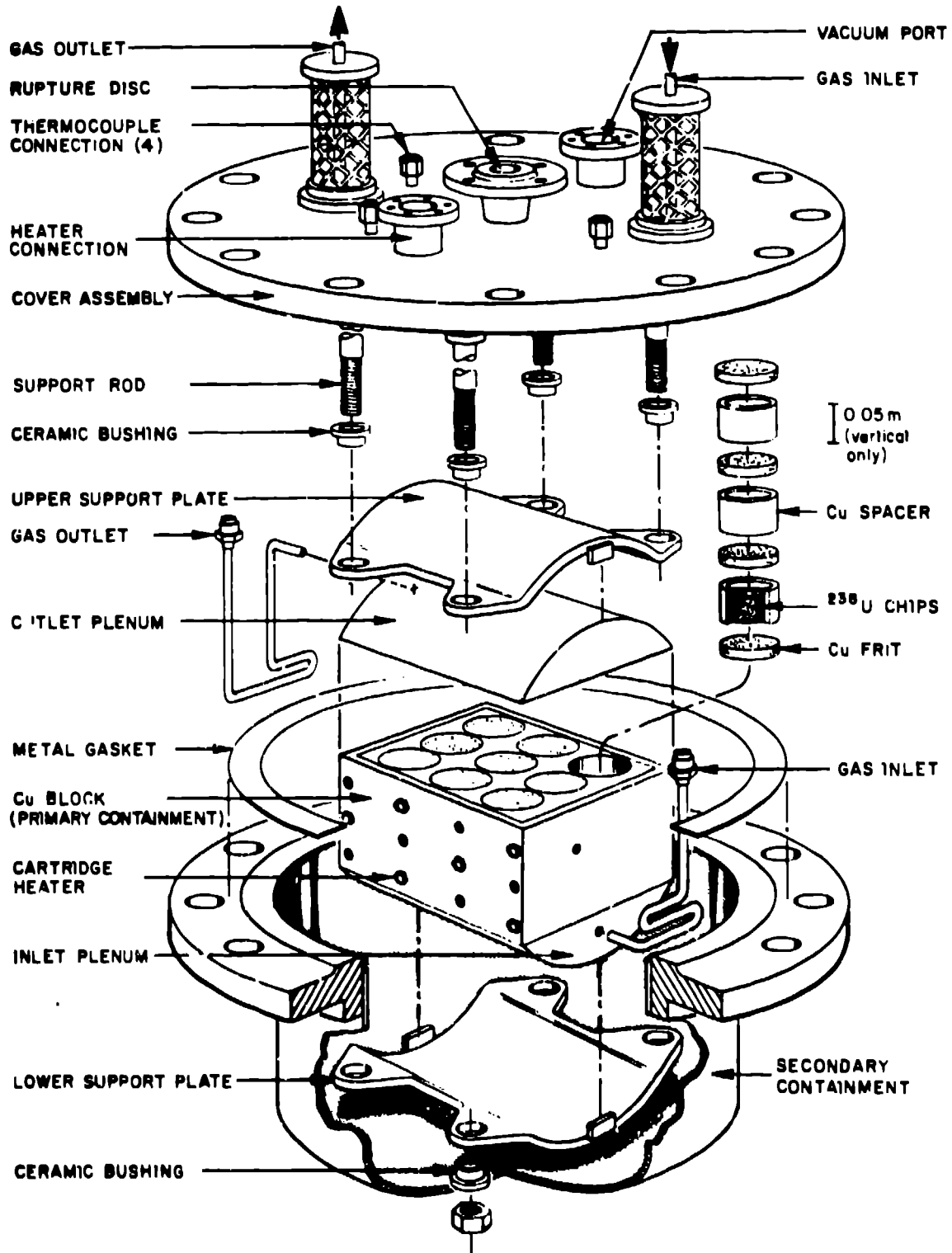


Fig. 3. Exploded view of the TSTA hydrogen storage bed.

TABLE 1 Parameter List for the TSTA Hydrogen Storage Bed

Total depleted uranium:	5.94 kg
Total number of cells:	27
Uranium in each cell:	0.22 kg
Theoretical T ₂ capacity:	0.2265 kg
Maximum T ₂ loading:	0.0906 kg
Per cent design capacity:	40
Number of heaters:	6
Heater power:	250 W (per heater)
Operational temperature range:	300-723°K
Maximum allowable pressure:	0.52 MPa
Maximum pressure rating:	0.69 MPa*
Primary container weight:	45 kg
Secondary container weight:	135 kg

*For secondary container.

pressure boundary is at the secondary container. The rupture disc is an additional safety feature in the event of overpressure caused by an unlikely event of air exposure of the uranium powder. The glovebox is inerted with nitrogen gas.

The storage bed will be qualified for TSTA use after several storage-recovery cycles with deuterium. The details of uranium-hydride-uranium cycle kinetics are well-documented in the literature. An experimental model of the TSTA storage bed has been built for experimental data and for mathematical model verification. (These models are not in the scope of this paper.) The next section provides a thermal analysis of the storage bed.

THERMAL BEHAVIOR ANALYSIS

The thermal behavior of the primary and the secondary system was analyzed for heat flow in the storage bed cartridge heater sizing, insulation selection, and operational temperatures. Because of the complex design, several simplifications and a conservative approach were used in the analysis. A 60% capacity (instead of design basis 40%) was used for conservatism.

Primary System Heating

The primary system heating during hydriding and dehydriding cycles is analyzed below. A thermal radiation analysis is also performed for heat losses from the primary system. In this section, we are looking for the maximum temperature in

the primary system so we neglect small heat losses that occur slowly from the primary container.

Hydriding Cycle Maximum Adiabatic Temperature Rise. An energy balance for the U-bed primary system (mainly, the ^{238}U powder and the copper block) with very rapid heating or no heat losses consists of the following equation for constant material properties.

$$Q_r = MC_p \Delta T, \quad (1)$$

where

Q_r = Heat input by hydriding,

M = Total mass of Cu and U,

C_p = Average specific heat at constant pressure,

and

ΔT = Change in temperature.

Also

$$Q_r = n[\Delta H(\text{UD}_3) + \Delta H(\text{UT}_3)]$$

where n is the number of moles of UD_3/UT_3 formed and $\Delta H(\text{UD}_3)$ and $\Delta H(\text{UT}_3)$ are heat of reaction for the UD_3 and UT_3 formation, respectively. Thus,

$$n = 7.5,$$

$$Q_r = 1.95 \text{ MJ},$$

$$M = 36.2 \text{ kg},$$

and

$$C_p = 343 \text{ J kg}^{-1} \text{ }^\circ\text{K}^{-1}.$$

A temperature rise (ΔT) of 157°K is calculated from Eq. (1) for the primary system. This calculation does not include heating of the inlet/outlet piping or heat losses to the secondary system (secondary container, primary container support, and flange and cover assembly). Therefore, 157°K is a conservative upper limit for the copper primary container temperature at the end of hydriding. However, hot spots exist at the uranium phase and at the copper walls touching the uranium. External heating of the bed may be necessary for desirable hydriding rates. The inlet and outlet piping (Fig. 3) that is made of 6.4-mm-thick SS 304 tubing has a very small conduction surface in contact with the primary container. Thus, heat losses through this path are very small. In addition, comparing thermal diffusivity of copper and SS 304, conduction will be about 24 times slower in SS 304 than in the same thickness of copper.

Radiative Losses in Hydriding. The radiative losses from the copper surfaces of the primary container to the SS 304 secondary container and the cover are estimated below for the hydriding cycle. For a reasonable approximation, the U-bed assembly (Fig. 3) may be considered as two concentric spheres.

The net radiative heat flux at the primary container is given by the following equation if the secondary container is filled with a nonparticipating medium (Ozisik, 1977).

$$q_1 = \frac{\sigma(T_1^4 - T_2^4)}{\frac{1}{\epsilon_1} + \left(\frac{A_1}{A_2}\right)\left(\frac{1}{\epsilon_2} - 1\right)}, \quad (2)$$

where σ is the Stefan-Boltzmann constant and A_1 and A_2 are the surface areas of the primary container and the secondary container, respectively. ϵ_1 and ϵ_2 are the emissivities of these surfaces at temperatures of T_1 and T_2 , respectively. The following assumptions are valid with this equation.

1. Radiative properties are uniform and independent of direction and wavelength.
2. Surfaces are diffuse emitters and diffuse reflectors.
3. The radiative heat flux leaving the surface is uniform over the surface of each container.
4. Surfaces are opaque.
5. Either a uniform temperature or a uniform heat flux is prescribed over the surface of each container.
6. The enclosure is filled with a nonparticipating medium such as a vacuum. (Gases such as nitrogen are relatively transparent to thermal radiation unless the temperature is extremely high).

Given $\epsilon_1 = 0.1$ (polished copper at 698°K);

$\epsilon_2 = 0.22$ (SS 304);

$T_1 = 443^\circ\text{K}$;

$T_2 = 300^\circ\text{K}$;

$\sigma = 5.6697 \times 10^{-8} \text{ W m}^{-2} \text{ }^\circ\text{K}^{-4}$;

$A_1 = 0.2 \text{ m}^2$; and

$A_2 = 0.53 \text{ m}^2$;

a radiation heat flux of 152.1 W m^{-2} is calculated from Eq. (2). After a quick temperature rise of 143°K in the primary container, 30.4 W is lost by radiation to the secondary container.

The inlet/outlet piping and the primary system support structure will in reality receive some amount of radiative heat flux. The primary system heating will cause heating of the inlet/outlet piping and the primary system support structure, and then heating of the secondary container. The highest temperature rise will occur in the primary system. The above analysis is a reasonably conservative picture of maximum temperatures and rate of cooling.

Heater Sizing. Similarly to the hydriding case, an energy balance for the primary system (^{238}U , UD_3 , UT_3 , and copper) with rapid heating (or no heat losses) consists of the following equation for constant material properties during dehydriding.

$$Q_c - Q_r = MC_p\Delta T, \quad (3)$$

where

Q_c = External heat input (provided by cartridge heaters),

Q_r = Heat of reaction for dehydriding

= 1.95 MJ,

M = Total mass of Cu, U, and UD_3/UT_3

= 39.9 kg,

and

C_p = 377 J kg^{-1} $^{\circ}\text{K}^{-1}$.

Thus, for a desired temperature increase, the cartridge heater power input can be calculated from Eq. (3). Table 2 summarizes various heating times for the primary system at 1500 and 150 W heating rates. The heat of reaction was varied as shown to identify the effect on the heating times. The cartridge heating rate of 1500 W looks reasonable for the requirement to heat the U-bed to 723°K in 1.5 h for the dehydriding process.

Radiative Losses in Dehydriding. The radiative loss from the copper surfaces of the primary container to the SS 304 lid and the secondary container are calculated from Eq. (2) in a manner that is similar to the hydriding case. At $T_1 = 723^{\circ}\text{K}$, $T_2 = 300^{\circ}\text{K}$, a heat flux of 1325.7 W m^{-2} is calculated. After an assumed sudden temperature rise to 723°K, 265.1 W is lost instantaneously by radiation to the secondary container, so the 150 W heating rate is inadequate.

Similarly to the hydriding phase, there will be conductive and radiative thermal losses from the primary container to the inlet/outlet piping, the primary system support structure, and the secondary container and cover assembly. The highest temperatures will be located in the primary container. The equilibrium primary container temperatures are expected to be less than 723°K because of these additional losses.

Heat Flow Analysis for Secondary Container

An analysis of the transient and steady-state heat flow conditions to and from the secondary container is provided below. We are now interested in the maximum

TABLE 2 Calculated Heating Times

	<u>1500 W</u>	<u>150 W</u>
Heating 300 → 723°K with ΔH_p	1.54 h	15.4 h
Heating 300 → 723°K without ΔH_p	1.18 h	11.8 h
Heating 300 → 473°K without ΔH_p , and 473 → 723°K with ΔH_p	0.48 h and 1.05 h	4.8 h and 10.5 h

heat flux from the primary to the secondary container to predict a conservatively high maximum temperature in the secondary container wall. First, a heat transfer coefficient for free convection in the nitrogen gas surrounding the U-bed secondary container in the glovebox is calculated for use in the subsequent analysis.

Free Convection. The average Nusselt number for free convection in nitrogen gas from the outer cylindrical surface of the secondary container (Fig. 3) can be calculated by comparison with a vertical plate (Cebeci, 1975). For $T_w = 318^\circ\text{K}$ (wall temperature), $T_f = 300^\circ\text{K}$ (fluid temperature), $P = 10^{-5}\text{Pa}$ (fluid pressure), and the fluid properties at the arithmetic mean of T_w and T_f , the Prandtl number (Pr), the Grashof number (Gr_L), and specific parameter ζ are evaluated to be the following.

$$Pr = \frac{C_p \mu}{k} = 0.71,$$

$$Gr_L = \frac{g\beta(T_w - T_f)L^3}{\nu^2} = 9.4 \times 10^6,$$

and

$$\zeta = \frac{2.7^2}{Gr_L^{0.25}} \left(\frac{L}{R}\right) = 0.07,$$

where C_p (specific heat), μ (viscosity), k (thermal conductivity), β (temperature coefficient of thermal conductivity), and ν (kinematic viscosity) are the fluid properties, and L and R are the height and radius of the vertical cylinder (secondary container). The free convection flow is in the laminar range because $Gr_L Pr = 6.7 \times 10^6$ (Ozisik, 1977). The ratio of the Nusselt number for a vertical cylinder to that for a vertical flat plate for laminar free convection at a uniform wall temperature is obtained from Cebeci (1975) to be 1.05. Thus, we can assume that the flat-plate correlation is applicable for the outside of the cylindrical U-bed secondary container. The average Nusselt number under uniform surface conditions is given by McAdams (1954).

$$Nu_m = 0.59 (Gr_L Pr)^{0.25}. \quad (4)$$

A mean Nusselt number of 30 is calculated from Eq. (4) over the height of the vertical cylinder. From $Nu_m = h_m L/k$, a mean heat-transfer coefficient (h_m) of $4.09 \text{ W m}^{-2} \text{ }^\circ\text{K}^{-1}$ is calculated for free convection in the nitrogen gas in the glovebox.

Transient Analysis. The Biot number ($Bi = hL/k$) is used to compare the relative magnitudes of the surface transfer coefficient (h) and the internal conductance of a slab to heat transfer. For values of Bi less than about 0.1, the temperature in a medium is essentially uniform at any given time. The spatial variation of temperature can be neglected for such cases. Then, the variation of temperature in the solid with time can be analyzed with lumped-system analysis (Ozisik, 1977). The transient heat flow from the primary container to the secondary container is analyzed below as a one-lump system with convection and with prescribed heat-flux boundaries as shown in Fig. 4. The analysis is valid because $Bi = 1.2 \times 10^{-3}$ for the secondary container wall.

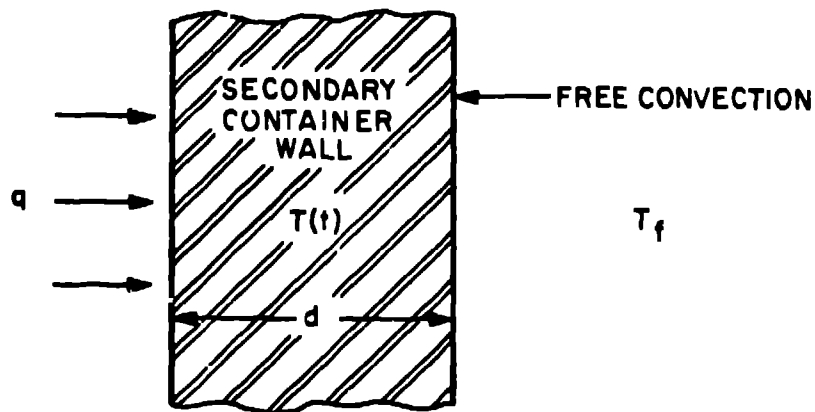


Fig. 4. One-lump analysis of transient heat flow in the secondary container wall with a heat supply at the inner surface and free convection from the outer surface.

An energy balance for the secondary container wall consists of the following equation.

$$A_i q + A_o h [T_f - T(t)] = \rho C_p V \frac{dT(t)}{dt}, \quad \text{for } t > 0$$

with the initial condition (I.C.)

$$T(t) = T_0, \quad \text{at } t = 0,$$

where q is the heat supply, A_i and A_o are the inner and outer surface area, ρ and C_p are the density and specific heat of the wall, and V is the wall volume.

Assuming constant ρ , C_p , h , and $A_i = A_o = A = \frac{V}{L}$,

$$q + h[T_f - T(t)] = \rho C_p L \frac{dT(t)}{dt},$$

which can be reduced to

$$\frac{d\theta(t)}{dt} + m\theta(t) = Q, \quad \text{for } t > 0 \quad (5)$$

$$\text{I.C. } \theta(t) = \theta_0 = T_0 - T_f, \quad \text{at } t = 0,$$

where

$$\theta(t) = T(t) - T_f,$$

$$m = \frac{h}{\rho C_p L},$$

and

$$Q = \frac{q}{\rho C_p L}.$$

The solution of Eq. (5) is the sum of the solution of the homogeneous part and a particular solution.

$$\theta(t) = C e^{-mt} + \theta_p, \quad \text{and}$$

$$\theta_0 = C + \frac{Q}{m}, \quad (\text{I.C.}).$$

Thus

$$\theta(t) = \theta_0 e^{-mt} + (1 - e^{-mt}) \frac{Q}{m},$$

which predicts the temperature variation of wall as a function of time. As $t \rightarrow \infty$, we can calculate the equilibrium temperature because

$$\theta(\infty) \rightarrow \frac{Q}{m} = \frac{q}{h}. \quad (6)$$

For the hydriding case discussed in the previous section, $q = 152.1 \text{ W m}^{-2}$ is the radiative heat flux leaving the primary container. An equilibrium secondary container wall temperature increase of 37.2°K is calculated from Eq. (6) without surface area correction. With correction for area, the incident flux on the secondary container is

$$q = 152.1 \times \frac{0.2}{0.53} = 57.4 \text{ W m}^{-2}, \text{ and}$$

the temperature rise is 14°K .

For dehydrating, the equilibrium temperature rise is 324.2°K for a flux leaving the primary at 1325.7 W m^{-2} . The incident flux on the secondary is 500.3 W m^{-2} with area correction and $\theta(\tau) = 122.3^\circ\text{K}$. A temperature rise of 14°K for hydriding and 122.3°K for dehydrating are higher estimates than would be expected for the secondary container wall because of the additional heat loss mechanisms.

Insulation Analysis. Although the above results indicate that the secondary container does not overheat, its surface temperature is important for the U-bed and glovebox operator. Therefore, the potential for reduction in temperature for the wall of the secondary container is discussed in this section.

A steady-state analysis of heat transfer from the primary container to the secondary container is given below for the dehydrating phase. This is needed because of higher temperatures at the secondary container during the dehydrating phase rather than during the hydriding phase. Figure 5 illustrates the geometry where $T_1 = 723^\circ\text{K}$, $T_f = 300^\circ\text{K}$. An average gap distance of 76 mm will be used in the following calculations. The gap will be filled with N_2 gas, Firelite 2200, Zeolite pellets with N_2 , evacuated Zeolite pellets, Celotex, and multilayer insulation (such as nickel foil) for a comparative analysis.

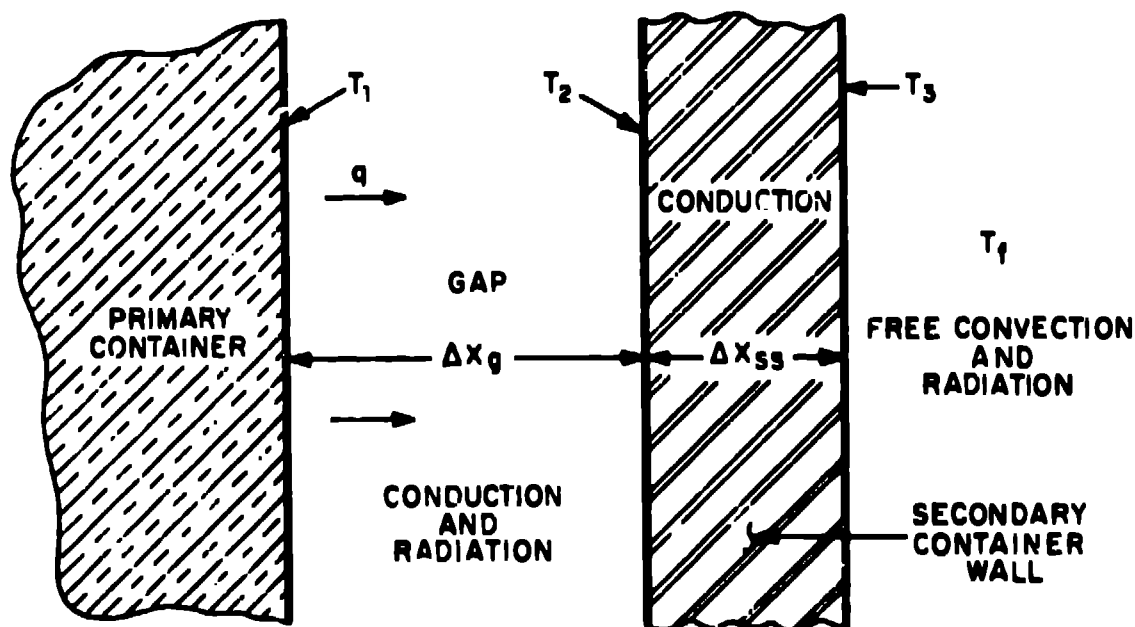


Fig. 5. Heat transfer modes for steady-state analysis.

Without the radiative component, the governing equations are as follows.

$$T_1 - T_2 = q \left(\frac{\Delta x_g}{k_g} \right), \quad (\text{for conduction in the gap}) \quad (7)$$

$$T_2 - T_3 = q \left(\frac{\Delta x_{SS}}{k_{SS}} \right), \quad (\text{for conduction in the wall}) \quad (8)$$

and

$$T_3 - T_f = q \left(\frac{1}{h_f} \right), \quad (\text{for convection from the wall}) \quad (9)$$

combined as

$$T_1 - T_f = q \left[\frac{\Delta x_g}{k_g} + \frac{\Delta x_{SS}}{k_{SS}} + \frac{1}{h_f} \right], \quad (10)$$

where

T_1 = Primary container surface temperature,

T_2 = Secondary container inner surface temperature,

T_3 = Secondary container outer surface temperature,

T_f = Nitrogen gas temperature,

q = Heat flux for conduction,

Δx_g = Gap distance,

Δx_{SS} = Secondary container wall thickness,

k_g = Gap thermal conductivity,

k_{SS} = Secondary container thermal conductivity,

and

h_f = Convective heat transfer coefficient.

Thus, for given values of Δx_g , Δx_{SS} , k_g , k_{SS} , and h_f , q is calculated from Eq. (10) for $T_1 = 723$ K and $T_f = 300$ K. Then, T_2 and T_3 are calculated from Eqs. (7) and (8), respectively. Table III lists the calculated heat flux (q) and the resulting surface temperature (T_3) for the secondary container with various media in the separation gap.

TABLE 3 Comparison of Various Gap Media for U-Bed Surface Temperatures for Dehydrating*

	$k_g(\text{W m}^{-1} \text{ }^\circ\text{K}^{-1})$	$q(\text{W m}^{-2})$	$T_3(\text{ }^\circ\text{K})$
N_2	0.042	206	350
Firelite 2200	0.22	722	470
Zeolite pellets in N_2	0.58	1140	575
Evacuated Zeolite pellets	0.0012	7	307
Celotex	0.089	387	394
Multilayer insulations	0.00015	0.8	300

*For conduction only.

The case for nitrogen is not complete without radiative heat transfer. Hence, the calculated temperature of 350°K is about 122°K less than what might result under conduction combined with radiation. Also, the multilayer insulation is not expected to work efficiently in the U-bed situation unless possible thermal shorting by the auxiliary components such as piping and instrumentation leads is avoided, the anisotropic nature of the insulation is minimized, and a vacuum service less than 13.3 mPa (10^{-4} torr) is provided (Long, 1972). It is possible to achieve a vacuum lower than 13.3 mPa with a 38-mm port from a 0.36-m chamber, as in this case. An estimate of the minimum pressure (P_{\min} in torr) can be made for infinite pumping case by the following equation (Gupta, 1976).

$$P_{\min} \geq 0.9 K_{av} \left(0.66 + \frac{1}{g'} \right),$$

where

K_{av} = Average system outgassing rate (torr \cdot cm $^{-2}$ s $^{-1}$)

and

$$g' = \frac{\text{tube diameter}}{\text{chamber diameter}}$$

$$= \frac{1}{9.75}$$

Thus, the U bed internals outgassing will determine the pressure level with pumping. If the outgassing rate is lower than 1.2×10^{-2} torr \cdot cm $^{-2}$ s $^{-1}$ (1.6×10^{-3} Pa \cdot m 2 s $^{-1}$), which is a reasonable rate because almost all surfaces are oxygen free copper and SS 304, then $P_{\min} = 13.3$ mPa is achievable.

Comparison of various methods of thermal design results in the following qualitative order of lowest U-bed secondary container surface temperatures: super insulation/evacuated powders, Celotex, evacuation, Firelite 2200, Zeolite in N_2 , and N_2 . However, when other requirements such as simplicity, cost, maintenance, and leak management are considered, a simple evacuation might be sufficient.

CONCLUSIONS

We have presented the design of a hydrogen storage bed to be used in TSTA at the Los Alamos National Laboratory. The storage bed will be used to store DT gas as $U(D,T)_3$ when it is required for the TSTA operations. We conclude with the following observations, as supported by our conservative evaluation of the bed thermal performance for 60% capacity.

1. Heating of the bed may be necessary for desirable hydriding rates. A detailed computer model and supporting experimental data should verify this.
2. The cartridge heating rate of 1500 W appears satisfactory for the requirement to heat the U-bed to 723 K in 1.5 h for the dehydriding process.
3. During hydriding, the primary system average temperature rises by 157°K. A maximum thermal radiation heat flux of 152 W m^{-2} from the primary system is calculated.
4. During dehydriding, a thermal radiation heat flux of 1326 W/m^2 from the primary system is calculated. The maximum total radiative heat loss is about 265 W.
5. Equilibrium secondary wall temperature increases for hydriding and dehydriding are less than 37 and 324 K, respectively.
6. During dehydriding, the lowest secondary wall temperatures are possible with evacuated powders or multilayer insulations.

ACKNOWLEDGEMENTS

We learned from the experiences of others. The most notable help came from the Lawrence Livermore National Laboratory, Sandia National Laboratories-Livermore, and, of course, the Los Alamos National Laboratory. Our sincere thanks are extended to all the people involved, with special thanks to J. L. Anderson and D. O. Coffin from Los Alamos.

This work was supported by the US Department of Energy, Office of Fusion Energy.

REFERENCES

- Anderson, J. L. (May 9-11, 1978). "The Tritium Systems Test Assembly at the Los Alamos Scientific Laboratory," Trans. of American Nuclear Society Third Topical Meeting on the Technology of Controlled Nuclear Fusion, p. 201.
- Celaci, T. (1975). "Laminar Free Convective Heat Transfer from the Outer Surface of a Vertical Slender Circular Cylinder," Fifth Int. Heat Transfer Conf., Vol. 3, NC 1.4, pp. 15-19.
- Gupta, A. K. (1976). "A Simplified and Comprehensive Approach to Vacuum System Estimates," Vacuum, Vol. 27, No. 1, p. 17.
- Hagel, W. C. and K. H. Wiska (August 25, 1980). "How to Select Alloy Steels for Pressure Vessels II," Chem. Eng. J., p. 105.
- Hansen, M. (1958). Constitution of Binary Alloys and (1965) First Supplement, McGraw Hill Book Company, New York.

Long, H. M. (1972). "The Industrial Application of Vacuum Installations," AIChE Symposium Series No. 125, Vol. 68, Am. Inst. Chem. Engrs.

McAdams, W. H. (1954). Heat Transmission, 3rd ed., McGraw-Hill Book Company, New York.

Mueller, W. M., J. P. Blackledge, and G. G. Libovitz (1968). Metal Hydrides, Academic Press, New York.

Ozisik, M. N. (1977). Basic Heat Transfer. McGraw-Hill Book Company, New York.

Singleton, M. F. and R. M. Alire (May 1980). "Traps for Scavenging Hydrogen Isotopes," Lawrence Livermore National Laboratory report UCRL-80443.